# An novel explicit model for photovoltaic I-V characteristic prediction based on different splitting spectrum

Luqing Liu[1,2]*, Wen Liu[1,2], Xinyu Zhang[1], Jan Ingenhoff[2]

[1]*Optics and Optical Engineering Department, USTC (University of Science and Technology), Hefei China*

[2]*Institute of Advanced Technology, Hefei China*

**Abstract:** Looking at different operating climatic conditions, the electrical behavior predicting photovoltaic modules gets very important. For the estimation of output power from photovoltaic (PV) plants this is a very essential and basic aspect. In this paper, the relationship between the I-V curve and the irradiation spectrum is discussed by combining the single diode model. An explicit elementary analytical model with two defined shape parameters is discussed and improved with three approximations and second order Taylor expansion. Then, the explicit elementary analytical model is investigated under varying conditions leveraging the four parameters $I_{ph}$, $I_0$, $R_s$ and $R_{sh}$ from the single diode model. The relationship between the physical parameters and the condition parameters are discussed and applied to extract the shape parameters at different scenarios. Considering the aging effect, the process of calculation to predict the I-V curve under different splitting spectra is simplified as follow: (1) two shape parameters are gotten from the I-V data at measurement reference conditions (MRC); (2) the short circuit current, open circuit voltage and shape parameters under any splitting spectrum can be calculated based on the relationship provided in article; (3) the performance of PV panel can be predicted with parameters. The validation of this model was experimentally proven leveraging monocrystalline silicon photovoltaic module with different splitting films. Results showed that the model accurately predicts the I-V characteristics for the examined PV modules at different irradiance spectra and cell temperatures. Moreover, the presented model performs superior compared to other investigated models when looking at accuracy and simplicity.

**Keywords:** photovoltaic panel; explicit model; spectrum splitting; I-V characteristic prediction; shape parameter

## 1. Introduction

Photovoltaic power generation technology was greatly improved and widely used all over the world since it's invented[1]. Because the photovoltaic cell can't utilize all the wavelengths of sunlight effectively, there are many applications of systems combining several kinds of photovoltaic cells to get a higher system efficiency. The idea of utilizing specific ranges of sunlight spectrum for various kinds of photovoltaic cells was firstly presented in 1955 by Jackson[2] and firstly experimentally demonstrated in 1978 by Moon et. al[3]. Many studies were carried out in this field to improve the efficiency of photovoltaic systems[4-7]. There are also many papers about Hybrid Photovoltaic (PV)-Thermoelectric (TE) systems which is another kind of splitting technology emerged in recent years. The PV-TE systems make part of solar radiation available for PV generating system[8]. The rest of solar radiation is concentrated on the TE system for producing electricity by the thermoelectric effect. Thus the PV-TE systems further reduce the heat at the solar cells and improve the efficiency of the whole systems[9,10]. Photovoltaic power generating systems are also combined with some

 doi:10.20944/preprints201808.0248.v1

concepts different than power generating systems. For example, a photovoltaic-greenhouse system had been proposed by Sonneveld et al[11,12]. In this case photosynthetically active radiation is transmitted through the film that is coated on the glass roof of green houses for plant growth. The film has a total reflection in the near infrared (NIR) region. Therefore, solar panels can leverage NIR that is reflected and concentrated for power generation. For the systems with different combinations, the spectra of beam splitting are quite diverse. This situation requests an effective and precise way to predict the I-V curve of the PV panel under different irradiation spectra.

To get the I-V curve for a PV panel, a circuital equivalent model is needed. Among the models which are used in the papers for PV panel simulation, the one diode equivalent representation model is more common than other models such as two/three diodes equivalent representation models. This single diode model is also well known as five-parameter model since the current-voltage (I-V) curve in this model is determined by five parameters[13-15].. The equation received directly from the single diode model is a transcendental equation that is implicit. Therefore, the exact analytic solution of I-V curve can't be obtained directly. Many approaches have been carried out to extract the parameters in the single diode model[16,17]. Because of the complexity of the implicit model, the calculation of the I-V curve normally requires the parameters from the manufacture data sheet and it takes more time to approach the output current with the voltage of PV cells or panels. Many methods of the analytical explicit model of I-V characteristic have been investigated in the last two decades[18-25]. One kind of these methods expressing the I-V characteristic based on the Lambert W-function. This method is an exact expression derived from the physical model[15,26]. The other methods are in terms of elementary approach. The models based on these methods are more widely used in the practical application because of their simplified form. Karmalkar et al. presented an explicit model with defined shape parameters. They combined the explicit models and the single diode model to identify the relationship between the five physical parameters and defined the shape parameters[18,21]. With this relationship, the five physical parameters can be calculated or numerically approximated with just few measurements. Furthermore, the whole I-V curve and maximum operating point of the PV panel can be determined without tracking the output current and voltage until open circuit from short circuit.

PV systems are used under different conditions considering mainly changing temperature and irradiation. It is well known that the efficiency of PV cells decreases with increasing temperature and decreasing light intensity. There are many studies discussing the mathematical model of this phenomenon. In PV systems with spectral separation, the spectral response of the solar cells is typically used only to determine the photocurrent[5]. The changing irradiation spectrum is converted into the changing light intensity so that the photocurrent can be obtained under different spectrum condition[27-29]. The relationship between the five parameters and operating conditions can be used to develop a model to predict the I-V curve. Yunpeng Zhang et al. put forward a flexible and reliable method leveraging a few measurement at measurement reference conditions. This method is convenient for the practical application with the changing physical parameters in the photovoltaic panel working life[30].

In this paper, we propose a simplified elementary method for a PV panel which can predict the I-V characteristic under varying spectral conditions with two defined shape parameters. This explicit expression was directly derived from a physical model and improves the reduction of errors compared to previous methods. The two defined shape parameters are expressed directly by the values at standard reference conditions (SRC) or measurement reference conditions (MRC) and the solar spectrum after separation. The relationship between shunt resistance and irradiation spectrum is discussed combining

Preprints (www.preprints.org) | NOT PEER-REVIEWED | Posted: 14 August 2018 doi:10.20944/preprints201808.0248.v1

the spectral response. Considering the aging effect, the process of calculation to predict the I-V curve under different splitting spectra is simplified as follow: (1) two shape parameters are gotten from the I-V data at measurement reference conditions (MRC); (2) the short circuit current, open circuit voltage and shape parameters under any splitting spectrum can be calculated based on the relationship provided in article; (3) the performance of PV panel can be predicted with parameters. At the end of paper, the model are validated through the experiments with seven kinds of films. The reliability of the model is proved by the result of the validation experiments.

The single diode model is discussed and simplified in part 2 and 3. Then the method is discussed in part 4 with varying conditions, especially with different spectrum splitting. The method is validated and the result of experiment is discussed in part 5.

## 2. Single diode model

The physical model of a solar cell in a solar panel can be described as a single diode model such as shown in Fig. 1. The model contains a light-induced current source, an ideal diode, a series resistance and a shunt resistance. The light-induced current source provides photocurrent when the irradiation reaches the surface of solar cells based on photoelectric conversion. As it is well known, this model has five parameters: photocurrent ($I_{ph}$), shunt resistance ($R_{sh}$), series resistance ($R_s$), saturation current under reverse bias ($I_0$) and the ideality factor of diode ($n$).

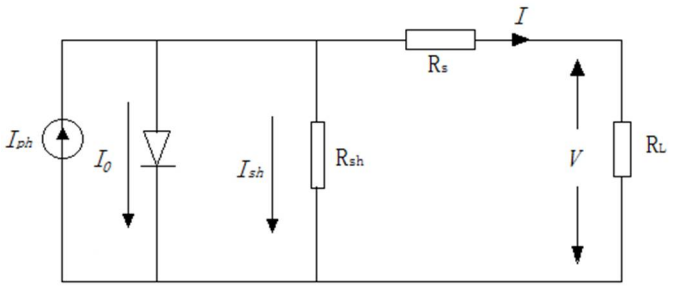


**Figure 1**. The equivalent single diode model for a PV panel or a solar cell

With those five parameters, the equation of I-V curve for a solar cell is:

$$I = I_{ph} - I_0(e^{\frac{V_{cell}+IR_{s,cell}}{nV_T}} - 1) - \frac{V_{cell}+IR_{s,cell}}{R_{sh,cell}} \quad (1)$$

In the equation (1), $V_T$ is equal to $kT/q$, in which $k$ is Boltzmann constant ($1.381\times10^{-23}$ J/K) and $q$ is the electronic charge ($1.608\times10^{-19}$ C). $T$ is the absolute temperature in Kelvin which is 298.15 K at SRC conditions. The parameters in the equation for a solar panel with $N_s$ identical solar cells in series can be modified as follow equations.

$$V = N_s V_{cell} \quad (2)$$

$$R_s = N_s R_{s,cell} \quad (3)$$

$$R_{sh} = N_s R_{sh,cell} \quad (4)$$

The equations (2) and (3) are suitable for varying kinds of solar cells, including monocrystalline silicon and polycrystalline silicon. In the series circuit, the total current is equal to the current of each component. Then equation of the I-V curve for a solar panel with $N_s$ identical solar cells in series

Preprints (www.preprints.org) | NOT PEER-REVIEWED | Posted: 14 August 2018 doi:10.20944/preprints201808.0248.v1

should be changed into the form as equation (5).

$$I = I_{ph} - I_0(e^{\frac{V+IR_s}{N_s n V_T}} - 1) - \frac{V + IR_s}{R_{sh}} \tag{5}$$

## 3. Explicit elementary analytical model with two defined shape parameters

Defining the normalized voltage $v$ and normalized current $i$ via the short circuit current $I_{sc}$ and open circuit voltage $V_{oc}$ derives in the following equations

$$v = V / V_{oc} \tag{6}$$

$$i = I / I_{sc} \tag{7}$$

Putting equation (5) and (6) into equation (7), the equation (7) can be expressed as follow:

$$i = 1 - \frac{I_0}{I_{sc}}[\exp(\frac{V + IR_s}{N_s n V_T}) - \exp(\frac{I_{sc} R_s}{N_s n V_T})] - \frac{(I - I_{sc})R_s + V}{R_{sh} I_{sc}} \tag{8}$$

To simplify the equation (8), three approximations are possible:

Ⅰ. Approximation 1 is about the term $\frac{(I - I_{sc})R_s}{R_{sh} I_{sc}}$.

Because the series resistance $R_s$ is much smaller than the shunt resistance in solar cells (normally $R_s/R_{sh} < 10^{-3}$ ), the term is far less than 1 and approximately equal to 0.

$$\frac{(I_{sc} - I)R_s}{I_{sc} R_{sh}} \le \frac{R_s}{R_{sh}} \ll 1 \tag{9}$$

Thus, this term can be ignored.

Ⅱ. Approximation 2 is about the term $\frac{I_0}{I_{sc}} \exp(\frac{I_{sc} R_s}{N_s n V_T})$

Considering short circuit condition with $V = 0$ and place it into equation (5), this part can be expressed as equation (10).

$$\frac{I_0}{I_{sc}} \exp(\frac{I_{sc} R_s}{N_s n V_T}) = \frac{I_0}{I_{sc}} - \frac{R_s}{R_{sh}} + (\frac{I_{ph}}{I_{sc}} - 1) < \frac{I_0}{I_{sc}} + \frac{I_{ph}}{I_{sc}} - 1 \tag{10}$$

For most solar cells, the value of saturation current is much lower than output current so that $I_0/I_{sc} << 1$ (normally $I_0/I_{sc} < 10^{-4}$ ). Furthermore, normally the value of $I_{ph}$ is approximately equal to the value of the output current $I_{sc}$. Therefore, we can get $I_{ph}/I_{sc} \approx 1$. Thus, this term can be approximately ignored

Preprints (www.preprints.org) | NOT PEER-REVIEWED | Posted: 14 August 2018 doi:10.20944/preprints201808.0248.v1

because of $\frac{I_0}{I_{sc}}\exp(\frac{I_{sc}R_s}{N_snV_T}) \ll 1$ .

Ⅲ. Approximation 3 is about the term $\frac{I_0}{I_{sc}}\exp(\frac{V+IR_s}{N_snV_T})$

Considering both short circuit condition and open circuit. Place $I = 0$ when $V = V_{oc}$ and $V = 0$ when $\mathbf{I} = \mathbf{I_{sc}}$ condition into equation (5), the form of the term $\frac{I_0}{I_{sc}}\exp(\frac{V+IR_s}{N_snV_T})$ can be transformed in the following way

$$\frac{I_0}{I_{sc}}\exp(\frac{V+IR_s}{N_snV_T}) \approx (1-\frac{V_{oc}}{I_{sc}R_{sh}})[\exp(v-1)]^{\frac{V_{oc}}{N_snV_T}\cdot(1-\frac{IR_s}{V_{oc}-V})} \tag{11}$$

After transforming into equation (11), the $(1-\frac{IR_s}{V_{oc}-V})$ is considered a voltage independent constant. The error caused by approximation 3 is the main error in this model. However, the error can be reduced by adjusting the expression of the term $\frac{V_{oc}}{N_snV_T}\cdot(1-\frac{IR_s}{V_{oc}-V})$

After these three approximations as shown above, the equation (8) can be changed into (12)

$$i = 1-\frac{V_{oc}}{R_{sh}I_{sc}}v-(1-\frac{V_{oc}}{I_{sc}R_{sh}})[\exp(v-1)]^{\frac{V_{oc}}{N_snV_T}\cdot(1-\frac{IR_s}{V_{oc}-V})} \tag{12}$$

Then it is easy to see that the equation (12) can be simplified with two defined parameters (linear parameter $\gamma$ and exponent parameter $m$) as follows:

$$i = 1-(1-\gamma)v-\gamma[\exp(v-1)]^m \tag{13}$$

The form of equation (13) can be simplified by a Taylor exponent expending row:

$$i = 1-(1-\gamma)v-\gamma[1+(v-1)+\frac{1}{2!}(v-1)^2+\frac{1}{3!}(v-1)^3...+\frac{1}{N!}(v-1)^N...]^m \tag{14}$$

If the equation (14) is approximated in the first order, it can be modified into equation (15).

$$i = 1-(1-\gamma)v-\gamma v^m \tag{15}$$

This form of the explicit I-V model is provided and discussed by Karmalkar et al. and allows an easy closed-form estimation of the entire I-V curve[18,31]. The predictability of this method was verified, and the scope was expanded to a wide range of solar cells made out of various materials[32]. The two

Preprints (www.preprints.org) | NOT PEER-REVIEWED | Posted: 14 August 2018 doi:10.20944/preprints201808.0248.v1

defined shape parameters can be derived from few measurement I-V points as well as five physical parameters in the single diode model. There is an explicit elementary expression with two shape parameters in this analyze method for the fill factor and the maximum power point. This method is proved that it fits better than the other methods for describing the performance of a PV panel[33]. The method can be widely used in practical applications because of the easy calculation avoiding the difficulty of measurements and numerical approaching in parameter extraction. This method can be improved by adding the second-order term in the Taylor expansion. In this way, the equation (13) can be changed into equation (16)

$$i = 1-(1-\gamma)v-\gamma(\frac{v^2+1}{2})^m \tag{16}$$

In this explicit analysis of I-V form, the normalized current $i_{mp}$ and normalized voltage $v_{mp}$ at maximum point can be gotten by:

$$\left.\frac{d(iv)}{di}\right|_{i=i_{mp}} = 0 \tag{17}$$

$$\left.\frac{d(iv)}{dv}\right|_{v=v_{mp}} = 0 \tag{18}$$

Then $i_{mp}$ and $v_{mp}$ are represented as follow:

$$v_{mp} = (m+1)^{-\frac{1}{m}} - 0.05(1-\gamma) \tag{19}$$

$$i_{mp} = 1-(1-\gamma)v_{mp}-\gamma(\frac{v_{mp}^2+1}{2})^m \tag{20}$$

The equation (16) ,(19) and (20) can express the I-V characteristic and maximum point with $I_{sc}$ and $V_{oc}$ while the $I_{sc}$ and $V_{oc}$ can be measured directly. Some manufacturers provide the five physical parameters of the solar cell at SRC. Of course, the two shape parameters $m$ and $\gamma$ can be extracted by the five physical parameters containing all the information of the I-V curve. The linear parameter $\gamma$ is defined by the equation (12) and (13) as:

$$\gamma = 1-\frac{V_{oc}}{I_{sc}R_{sh}} \tag{21}$$

The exponent parameter $m$ is defined in approximation 3 (see above) and the value can be determined by the derivative at the open-circuit point of the I-V curve to reduce the error as this has been mentioned in Karmalkar S,(2008).

$$\left.\frac{I_{sc}}{V_{oc}}\frac{di}{dv}\right|_{i=0} = \left.\frac{dI}{dV}\right|_{I=0} \tag{22}$$

Preprints (www.preprints.org) | NOT PEER-REVIEWED | Posted: 14 August 2018 doi:10.20944/preprints201808.0248.v1

Putting the equations (5) and (16) into the equation (22), the expression of $m$ is as follows

$$m = 1 - \frac{1}{\gamma} + \frac{V_{oc}}{N_s n V_T + \gamma I_{sc} R_s} \tag{23}$$

Furthermore, the value of $m$ is adjusted by a calibration parameter $\theta$ in the explicit model of Karmalkar (2008,2009)[18,31] in order to reduce the error which can't be avoided between the implicit model and the explicit model. The expression for the parameter $m$ with $\theta$ was changed into the equation (24).

$$m = 1 - \frac{1}{\gamma} + \frac{V_{oc}}{N_s n V_T + \theta\gamma I_{sc} R_s} \tag{24}$$

$\theta$ is an empirical value without any physical meaning and the value can be approximately represented by $\theta \approx 0.77 i_{mp}\gamma$. The expression contains current ratio at the maximum power point $i_{mp}$ so it can't be used for the prediction. Considering both short circuit condition and open circuit in the equations (5), $I_{sc}$ and $V_{oc}$ are expressed by the five physical parameters in the forms as follow:

$$I_{sc} \approx I_{ph}(1 + \frac{R_s}{R_{sh}})^{-1} \tag{25}$$

$$V_{oc} \approx N_s n V_T \ln[\frac{I_{ph}}{I_0} - \frac{N_s n V_T}{R_{sh} I_0} \ln(\frac{I_{ph}}{I_0})] \tag{26}$$

## 4. Explicit elementary analytical under varying conditions

In the single diode model, four parameters $I_{ph}$, $I_0$ ,$R_s$ and $R_{sh}$ are considered to be related to temperature and irradiation intensity. By defining the ratio of these four parameters at different conditions with varying temperature and irradiation, the following equations result :

$$K_{ph} = \frac{I_{ph}}{I_{ph}^{MRC}} \tag{27}$$

$$K_0 = \frac{I_0}{I_0^{MRC}} \tag{28}$$

$$K_{sh} = \frac{R_{sh}}{R_{sh}^{MRC}} \tag{29}$$

$$K_s = \frac{R_s}{R_s^{MRC}} \tag{30}$$

the expression of short-circuit current $I_{sc,}$, open-circuit voltage $V_{oc}$ and two shape parameters $m$ and $\gamma$ can be changed into equations (31)-(34) deriving from equations (21), (23),(25),(26) with the value of parameters at MRC and equations (27)-(30).

Preprints (www.preprints.org) | NOT PEER-REVIEWED | Posted: 14 August 2018 doi:10.20944/preprints201808.0248.v1

$$I_{sc} \approx K_{ph} I_{sc}^{MRC} \tag{31}$$

$$V_{oc} \approx \frac{T}{T^{MRC}} V_{oc}^{MRC} + N_s n V_T (\ln K_{ph} - \ln K_0) \tag{32}$$

$$\gamma = 1 - \frac{V_{oc}}{K_{ph} K_{sh} V_{oc}^{MRC}} (1 - \gamma^{MRC}) \tag{33}$$

$$m = 1 - \frac{1}{\gamma} - \frac{V_{oc}}{N_s n V_T (1 - K_s K_{ph} \frac{T}{T^{MRC}}) + \frac{K_s K_{ph} V_{oc}^{MRC} \gamma^{MRC}}{\gamma^{MRC} m^{MRC} + 1 - \gamma^{MRC}}} \tag{34}$$

The short-circuit current $I_{sc}^{MRC}$ and the open-circuit voltage $V_{oc}^{MRC}$ at MRC can be measured directly. Considering that the physical parameters can be changed during the working life[33], the shape parameters $m^{MRC}$ and $\gamma^{MRC}$ at MRC are extracted by two simple measurements of $i$ for $v = 0.4$ and $v$ for $i = 0.4$ which are chosen differently with Karmalkar S (2008) because of $(v^2+1)/2>v$.

$$\gamma^{MRC} = (i_{v=0.4} - 0.6) / 0.4 \tag{35}$$

$$m^{MRC} = \ln[\frac{0.6}{\gamma^{MRC}} + (1 - \frac{1}{\gamma^{MRC}}) v_{i=0.4}] / \ln(\frac{v_{i=0.4}^2 + 1}{2}) \tag{36}$$

Therefore, by using equations (35) and (36), there is only one parameter $n$ to identify the I-V curve under varying conditions. The parameter $n$ is independent of the temperature and irradiation, so it can be received from the datasheet provided by manufacturers as well as the I-V curve at MRC[32].

$$n = \frac{V_{oc}^{MRC}}{V_T^{MRC}} \left( \frac{v_{mp}^{MRC} - \frac{i_{mp}^{MRC}}{1 - \gamma^{MRC} + m^{MRC} \gamma^{MRC}} - 1}{m^{MRC} \ln v_{mp}^{MRC} + i_{mp}^{MRC} / \gamma^{MRC}} \right) \tag{37}$$

The maximum point $(v_{mp}^{MRC}, i_{mp}^{MRC})$ at MRC can be extracted by the formula (19), (20) and the measurements at MRC. Therefore, the identification of I-V characteristic at varying conditions is turned into how to obtain the relationship of the physical parameters between MRC and varying conditions.

When the spectra of the irradiation are different because of the spectral separation $Spl(\lambda)$ in power generating systems, the changing must be considered with the spectrum response of the solar panels $Rs(\lambda)$ and the solar irradiation spectrum $S(\lambda)$. The spectral ratio parameter $k_1$ is defined as follow:

$$k_1 = \frac{\int Spe(\lambda) Spl(\lambda) Rs(\lambda) d\lambda}{\int Spe(\lambda) Rs(\lambda) d\lambda} \tag{38}$$

the ratio of the photocurrent ($K_{ph}$) and the ratio of the saturation current($K_0$) can be extracted with the temperature[34].

Preprints (www.preprints.org) | NOT PEER-REVIEWED | Posted: 14 August 2018 doi:10.20944/preprints201808.0248.v1

$$K_{ph} = k_1 \cdot \frac{S}{S^{MRC}} \cdot \frac{1+\alpha_{ph}(T - T^{SRC})}{1+\alpha_{ph}(T^{MRC} - T^{SRC})} \tag{39}$$

$$K_0 = \left(\frac{T}{T^{MRC}}\right)^3 \exp\left(\frac{E_g^{MRC}}{kT^{MRC}} - \frac{E_g}{kT}\right) \tag{40}$$

In equations (39), the slope of the short-current and temperature $\alpha_{ph}$ can be extracted by the slope of voltage and temperature $\beta_{oc}$ which both are provided by some manufacturers.

$$\alpha_{ph} \approx \frac{1}{N_s n V_T^{MRC}} \left(\frac{V^{MRC}}{T^{MRC}} + \beta_{oc}\right) \tag{41}$$

In equations (39), $E_g$ is the band gap of the solar cell materials and exhibits a small temperature dependence. For silicon, $E_g$ can be represented as shown in Soto W D et al.(2006)[34]

$$E_g(T) = E_g(0) - \frac{\alpha_E T^2}{T + \beta} \tag{42}$$

where the $E_g(0)$ = 1.166 eV, $\alpha_E$ = 0.473 meV/K and $\beta$ = 636 K (Zeghbroeck, 2011).

For the shunt resistance of the solar cells, the ratio $K_{sh}$ is used to be considered as $S^{MRC}/S$ [22,24]. But some papers show that most of the shunts are process-induced, such as edge shunts, cracks, holes, scratches or aluminum particles, rather than material induced shunts [37,38]. These effects depend on the carrier in the solar cells related to the irradiation spectrum and the spectral response. In Ruschel C S (2016)[38], the relationship between shunt resistance and irradiation intensity of solar cells made from various materials are presented in different ways. At monocrystalline fitting conditions, the ratio expression for shunt resistance $K_{sh}$ with different irradiation spectra can be expressed as follows:

$$K_{sh} = \left(k_1 \frac{S}{S^{MRC}}\right)^{-0.9} \tag{43}$$

In many papers, the series resistance $R_s$ is considered as a constant which is independent of the temperature and irradiation. However, some researches show that series resistance decreases with irradiation intensity [39,40]. The expression of the relationship between $R_s$ and $S$ hasn't been provided in these papers, so it should be discussed and simulated before any prediction is done.

## 5.Validation

The validation experiments were performed with a monocrystalline silicon photovoltaic module. It was composed of 8 photovoltaic cells connected in series. The size of the photovoltaic cells was 12.5 cm× 12.5 cm and were provided by company Sun power. The I-V curve data were measured by Prova-210 measurement-equipment which can scan the I-V curve automatically in one minute. The uncertainty of current is 0.01 A and the uncertainty of voltage is 0.01 V. The solar irradiation and the temperature was monitored with a TES-1333 pyranometer and an infrared thermometer. The measurement error of the TES-1333 pyranameter is 10 W/m$^2$. The measurement error of infrared thermometer is 1 K.

The experiments were done with sun irradiation at 10 a.m. in November 23, 2017. The I-V curve for the photovoltaic module without film was measured with G = 880 W/m$^2$ and T = 285 K. The parameters on MRC condition $V_{oc}^{MRC}$, $I_{sc}^{MRC}$, $V_{i=0.4}$ and $I_{v=0.4}$ can be derived from the I-V curve directly.

Preprints (www.preprints.org) | NOT PEER-REVIEWED | Posted: 14 August 2018 doi:10.20944/preprints201808.0248.v1

The $m^{MRC}$ and $\gamma^{MRC}$ can be extracted from equations (35) and (36) with the corresponding shape parameters. The shape parameters of the measurement data at MRC conditions are listed in Table 1. It can be verified in Figure. 2 that the improved model with second order approximation is more accurate than the model with first order approximation as discussed in Karmalkar (2008).

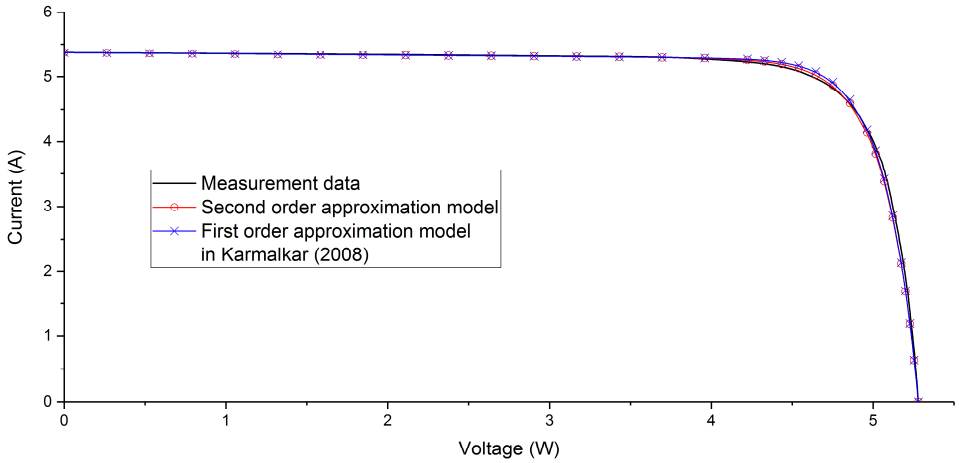


**Figure 2.** The I-V curve with measurement data, simulated data of improved model and simulated data of model in Karmalkar (2008)

**Table 1**

Shape parameters of measurement data at MRC of S = 880 W/m$^2$, T = 285 K

| Shape Parameters | Value |
|---|---|
| Short-circuit current $I_{sc}$ (A) | 5.368 |
| Open-circuit voltage $V_{oc}$ (V) | 5.280 |
| Exponent parameter $m$ | 24.58 |
| Linear parameter $\gamma$ | 0.982 |

There were seven kinds of films used in the experiments. The transmission spectra of the films are shown in Figure. 3. The spectral ratio parameter $k_1$, the temperature $T$ and the solar irradiation intensity $S$ of the reference condition for each film are listed in Table 3.

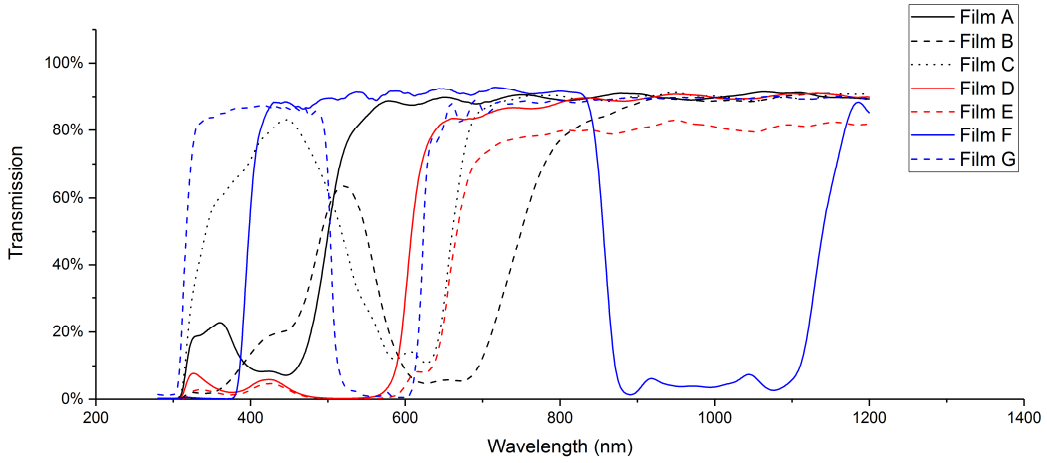


**Figure 3.** The transmission spectrum of the films used in the experiment

Preprints (www.preprints.org) | NOT PEER-REVIEWED | Posted: 14 August 2018 doi:10.20944/preprints201808.0248.v1

The decrease of series resistance $R_s$ is attributed to the increase in conductivity of the active layer. It is caused by the increase of the carriers with the increase in the intensity of illumination. So, the series resistance $R_s$ depend on the term $k_1 \frac{S}{S^{MRC}}$. The relationship is calculated using Matlab software as shown in Fig. 4. The equation (44), in which a = 0.04527 Ω and b = -1.26, is proven to be well consistent with the $R_s$ whose regression coefficient is 0.99. The value of the index parameter b is quite different with the value presented in Reich et al. (2009).

$$R_s = a(k_1 \frac{S}{S^{MRC}})^b \tag{44}$$

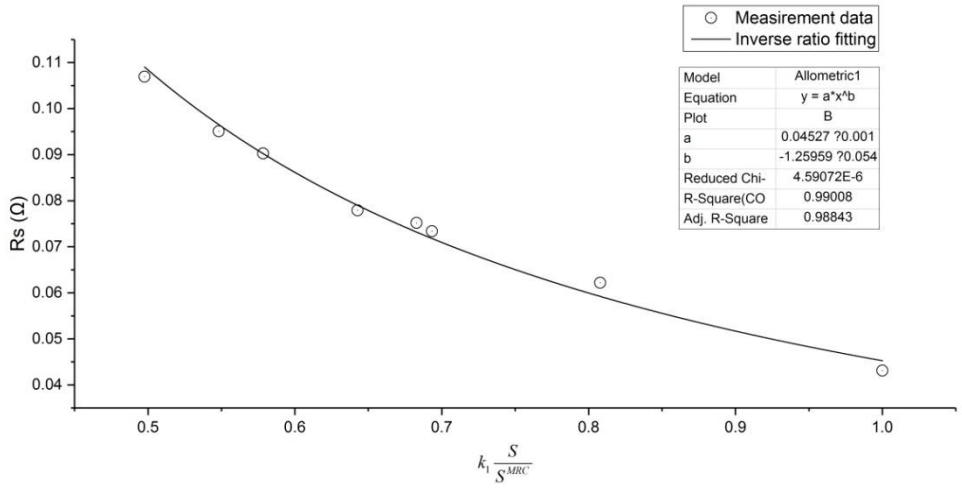


**Figure 4.** The relationship between $R_s$ and $k_1 \frac{S}{S^{MRC}}$ with inverse fitting ratio

The I-V curves and P-V curves of measurement data are shown in Figure.5(a) and Figure.5(b). As demonstrated, the output of the solar cells increase with the increase of spectral ratio parameter $k_1$. The only abnormal one is the measurement data of film F. It is because that the solar irradiation identity of film F measurement data is much lower than the others.

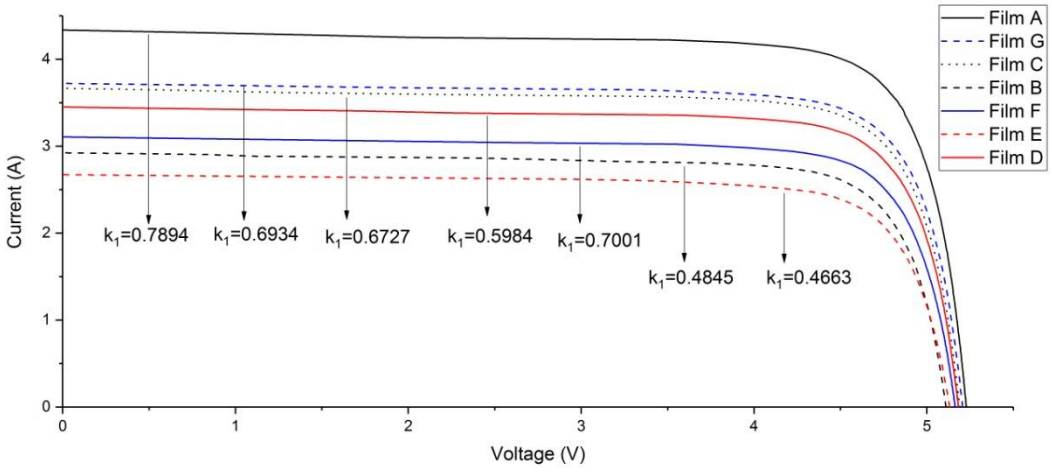


**Figure 5(a).** The I-V curves of film A-G with measurement data

Preprints (www.preprints.org) | NOT PEER-REVIEWED | Posted: 14 August 2018 doi:10.20944/preprints201808.0248.v1

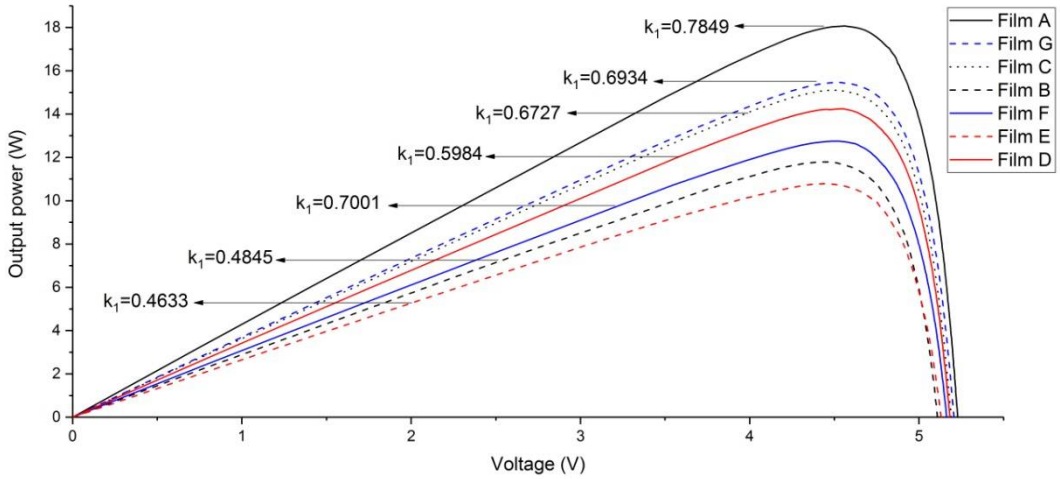


**Figure 5(b).** The P-V curves of film A-G with measurement data

**Table 2**

The proportional parameter $k_1$, the irradiation $S$, the temperature $T$ and the series resistance $R_s$.

| Film | $k_1$ | S(W/m$^2$) | T(K) | $R_s$(Ω) |
|---|---|---|---|---|
| A | 0.7894 | 900 | 286 | 0.06217 |
| B | 0.4845 | 989 | 287 | 0.09505 |
| C | 0.6727 | 893 | 291 | 0.07518 |
| D | 0.5984 | 945 | 296 | 0.07789 |
| E | 0.4633 | 945 | 294 | 0.10695 |
| F | 0.7001 | 807 | 301 | 0.09026 |
| G | 0.6934 | 896 | 295 | 0.07338 |

The prediction of the I-V curve and P-V curve for the film as it was calculated and discussed by our improved model shown above is compared with the prediction as calculated model in Yunpeng (2017) which used the explicit expression proposed in Karmalkar (2008,2009).

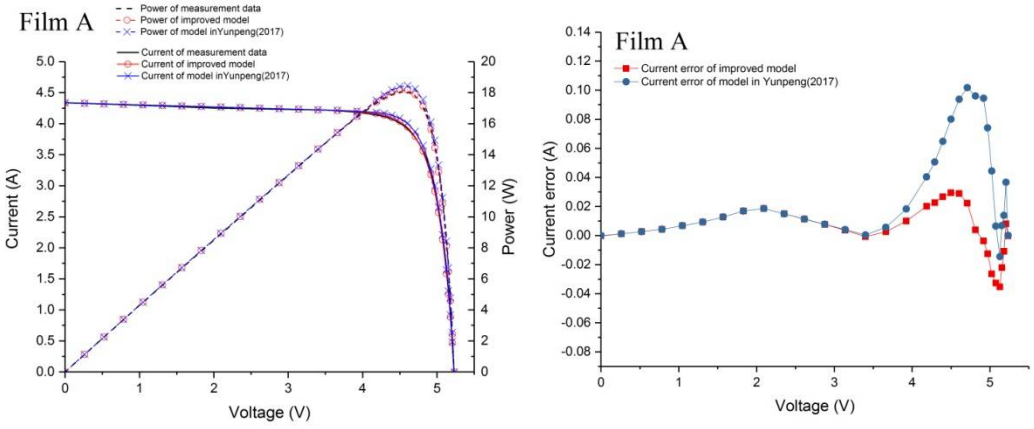


Figure 6(a) Figure 6(b)

**Figure 6.** The curves of film A with measurement data, fitted by improved model and model in Yunpeng (2017)(**a**); The current error curves of two models are also shown in the figure(**b**)

Preprints (www.preprints.org) | NOT PEER-REVIEWED | Posted: 14 August 2018 doi:10.20944/preprints201808.0248.v1

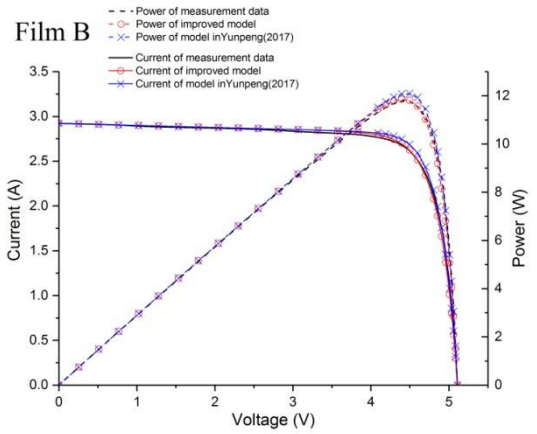


Figure 7(a)

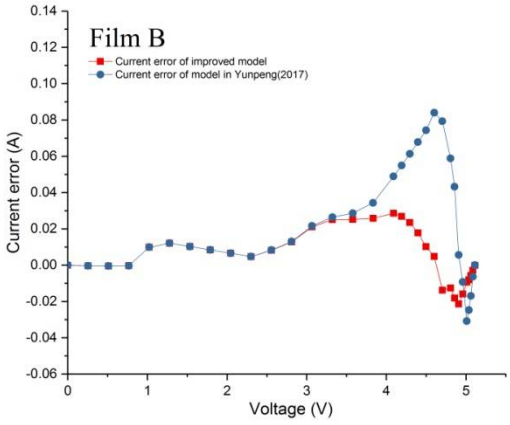


Figure 7(b)

**Figure 7.** The curves of film B with measurement data, fitted by improved model and model in Yunpeng (2017)(**a**); The current error curves of two models are also shown in the figure(**b**)

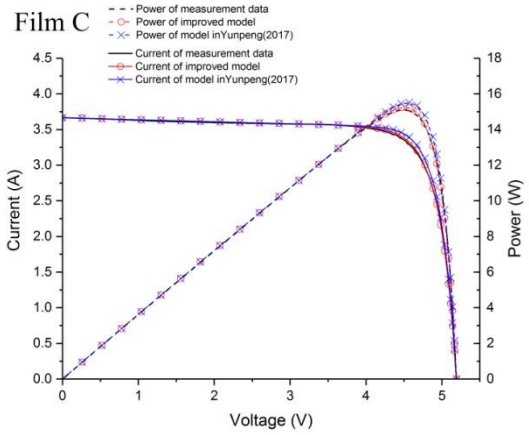


Figure 8(a)

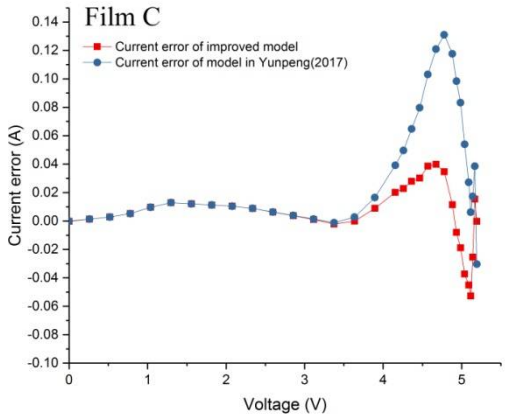


Figure 8(b)

**Figure 8.** The curves of film C with measurement data, fitted by improved model and model in Yunpeng (2017)(**a**); The current error curves of two models are also shown in the figure(**b**)

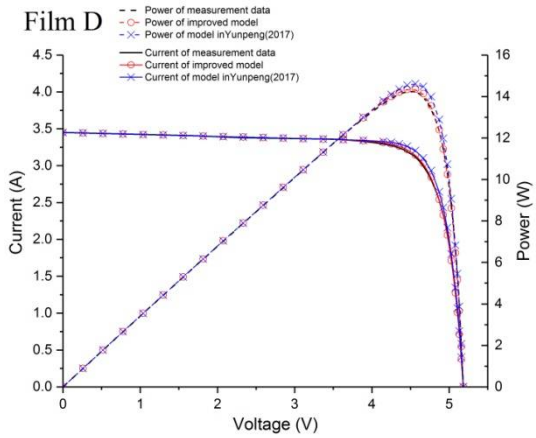


Figure 9(a)

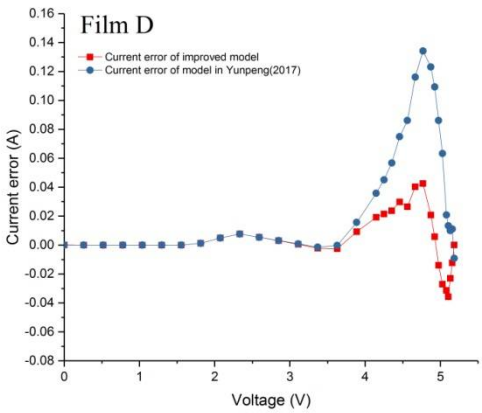


Figure 9(b)

**Figure 9.** The curves of film D with measurement data, fitted by improved model and model in Yunpeng (2017)(**a**); The current error curves of two models are also shown in the figure(**b**)

Preprints (www.preprints.org) | NOT PEER-REVIEWED | Posted: 14 August 2018 doi:10.20944/preprints201808.0248.v1

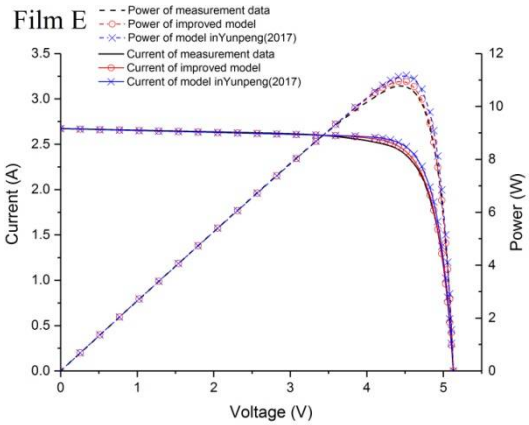


Figure 10(a)

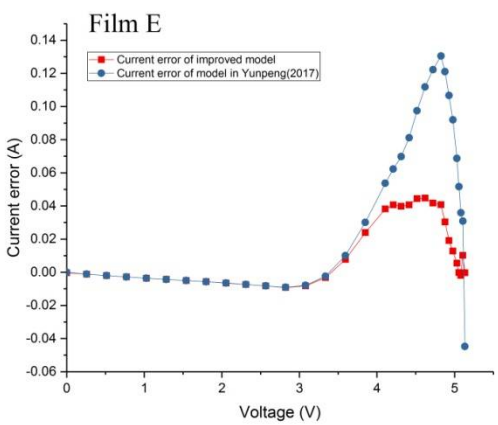


Figure 10(b)

**Figure 10.** The curves of film E with measurement data, fitted by improved model and model in Yunpeng (2017)(**a**); The current error curves of two models are also shown in the figure(**b**)

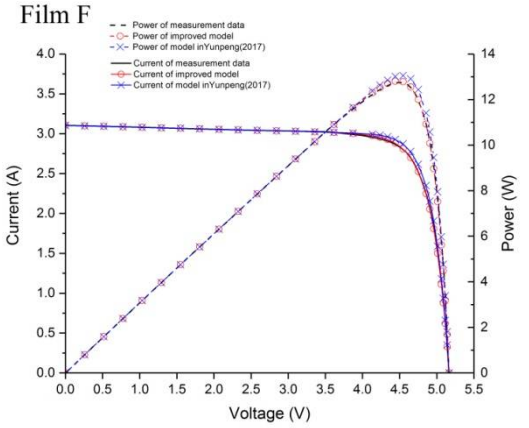


Figure 11(a)

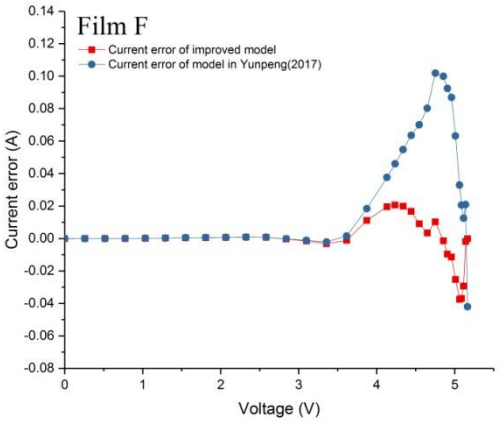


Figure 11(b)

**Figure 11.** The curves of film F with measurement data, fitted by improved model and model in Yunpeng (2017)(**a**); The current error curves of two models are also shown in the figure(**b**)

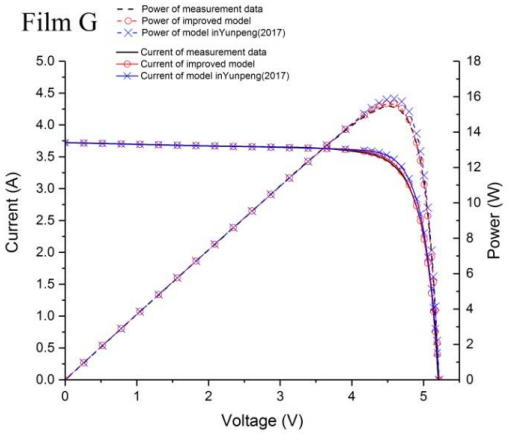


Figure 12(a)

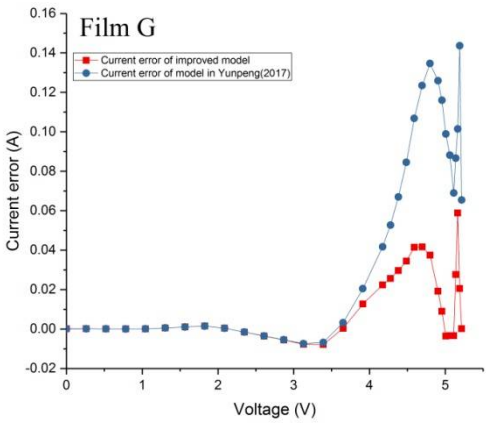


Figure 12(b)

**Figure 12.** The curves of film G with measurement data, fitted by improved model and model in Yunpeng (2017)(**a**); The current error curves of two models are also shown in the figure(**b**)

Preprints (www.preprints.org) | NOT PEER-REVIEWED | Posted: 14 August 2018 doi:10.20944/preprints201808.0248.v1

In Figure. 6-12, the I-V curves and P-V curves of the films A-G with corresponding measurement data are compared with the improved model and the model in Yunpeng (2017). The current error curves are also shown in figures. From the figures it gets clear, that the improved model is reliable enough to predict the I-V curve and P-V curve under different irradiation spectra. Thus, the effect of the irradiation spectrum and intensity on the parameters depends on the number of carriers. The error of the temperature and irradiation intensity measurement data causes the error of the I-V and P-V curve as well as the error of $V_{i=0.6}$ and $I_{v=0.6}$ extracted from the I-V curve at MRC. It can be concluded that the improved model has less error than the model in Yunpeng (2017) especially around the maximum power point. It means that the improved model has better predictability for the maximum power ($P_m$).

**Table 3**

Parameter *m* and maximum power of films A-G with measurement data, improved model and model in Yunpeng (2017)

| | Parameter *m* | | | Maximum power $P_m$ (W) | | |
|---|---|---|---|---|---|---|
| | Measurement data | Improved model | Model in Yunpeng(2017) | Measurement data | Improved model | Model in Yunpeng(2017) |
| Film A | 24.14 | 23.84 | 24.77 | 18.06 | 18.17 | 18.46 |
| Film B | 22.18 | 22.77 | 25.48 | 11.79 | 11.96 | 12.21 |
| Film C | 23.45 | 23.69 | 25.11 | 15.10 | 15.23 | 15.51 |
| Film D | 23.98 | 24.67 | 26.22 | 14.24 | 14.35 | 14.62 |
| Film E | 22.31 | 23.86 | 25.61 | 10.78 | 11.11 | 11.33 |
| Film F | 22.94 | 23.72 | 25.39 | 12.75 | 12.82 | 13.13 |
| Film G | 23.55 | 23.70 | 25.08 | 15.47 | 15.60 | 15.89 |

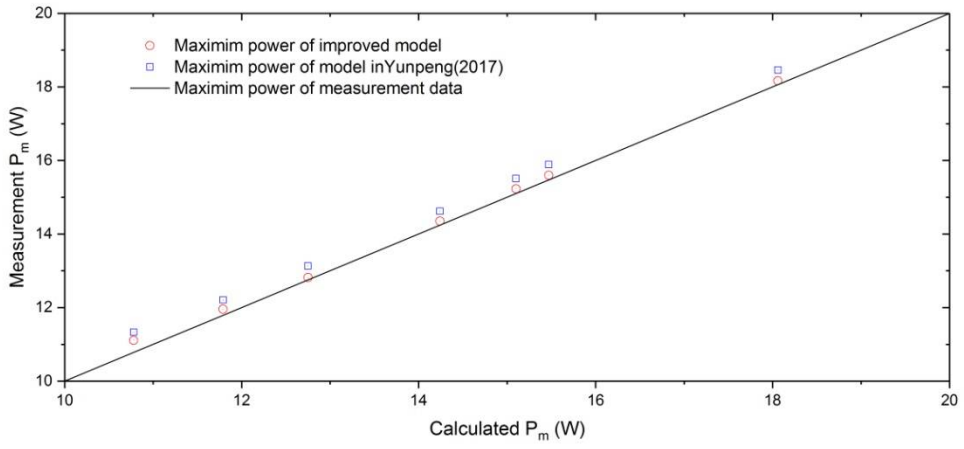


**Figure 13**. Maximum power of film A-G with measurement data, simulated data of improved model and simulated data of model in Yunpeng(2017)

In Fig. 13, the calculated parameter $P_m$ deriving from the improved model and the model in Yunpeng (2017) are compared with the measurement data. The error is primarily caused by the approximation 3 (see above) with the definition of shape parameters *m* and the approximation of equation (13) after the Taylor expansion. The error caused by the exponential term with *v* approaches 1 or 0 is not as high as around the maximum power point. In the improved model, the exponential term in the explicit expression is two orders of magnitude approximated instead of just the first order approximation as

 doi:10.20944/preprints201808.0248.v1

used in the explicit model of Karmalkar (2008,2009). Furthermore in Yunpeng(2017), the error is also caused by the value of $R_s$ which considered as a constant independency on the irradiation intensity. In the improved explicit model, the value of $R_s$ is well fitted so that the value of parameter $m$ is more accurate as shown in Table 4.

## 6. Conclusion

In this paper we present an explicit I-V model for a PV panel based on the single diode model under different irradiation spectra. The power law of I-V curves which are presented in Karmalkar (2008,2009) are discussed and calculated combining the single diode model with three approximations. The explicit analyze model is improved as a simple elementary term with second order approximation. To apply the model to the photovoltaic system with spectral separating, the spectrum of the irradiation is taken into account in the model as well. A spectral ratio parameter $k_1$ extracted from the irradiation spectrum, the transmission spectrum of the film and the spectral response of photovoltaic cells itself are set as a conditional parameter as well as temperature and irradiation intensity. The relationship between the physical parameters and the conditional parameters are discussed and applied to extract the shape parameters at different scenarios. The relationship between $R_s$ and the irradiation intensity as well as the spectrum are discussed and simulated. Furthermore, the condition parameters are used in the explicit analyze model directly to avoid the complex calculation and numerical approximation for the physical parameters as it was done in the single diode model. To avoid the aging effect, the measured I-V parameters from MRC are leveraged instead of the data from SRC, which are provided by the manufacturer. the process of calculation to predict the I-V curve under different splitting spectra is simplified as follow: (1) two shape parameters are gotten from the I-V data at measurement reference conditions (MRC); (2) the short circuit current, open circuit voltage and shape parameters under any splitting spectrum can be calculated based on the relationship provided in article; (3) the performance of PV panel can be predicted with parameters. In the validation experiments, the photovoltaic panel is tested with seven kinds of films. The experimental results showed that there is a good agreement between the calculated and measured I-V curve. The simple elementary term with second order approximation is proved better than the term in Karmalkar S (2008) and Karmalkar S (2009). Furthermore, the improved model has a better prediction of the maximum power compared to the model in Yunpeng (2017). Because of the advantages mentioned above, this model can be widely used for the prediction of I-V characteristic of a PV panel. This model is especially useful for a spectrum splitting system, such as system with various kinds of photovoltaic cells, some kinds of Hybrid Photovoltaic (PV)-Thermoelectric (TE) systems, solar cells used in agriculture and architecture. For the simplicity and validated predictability, this model can be used to design a monitoring software forecast the I-V characteristic for a photovoltaic panel used in a PV system for a long time.

**Author Contribution**: Investigation, Luqing Liu and Wen Liu; Simulation, Luqing Liu; Validation experiments, Luqing Liu and Xinyu Zhang; Writing Luqing Liu and Jan Ingenhoff

**Acknowledge**: This work was supported by the horizontal project between the government of Fuyang city and Teacher college of Fuyang. The project ID is XDHX201724. The measurement of film spectra was done by the Experimental center of USTC(University of Science and Technology of China).

 doi:10.20944/preprints201808.0248.v1

**Conflicts of Interest**: The authors declare no conflict of interest.

## Nomenclature

| | |
|---|---|
| $I_{ph}$ | photocurrent |
| $R_{sh}$ | shunt resistance |
| $R_s$ | series resistance |
| $I_0$ | saturation current |
| $n$ | ideality factor of diode |
| $V_{cell}$ | voltage of solar cell |
| $R_{s,cell}$ | series resistance of solar cell |
| $R_{sh,cell}$ | shunt resistance of solar cell |
| $V_T$ | thermal voltage |
| $T$ | absolute temperature |
| $k$ | Boltzmann constant |
| $q$ | electronic charge |
| $N_s$ | Number of solar cells in series |
| $v$ | normalized voltage |
| $i$ | normalized current |
| $V_{oc}$ | open circuit voltage |
| $I_{sc}$ | short circuit current |
| $\gamma$ | linear parameter |
| $m$ | exponent parameter |
| $i_{mp}$ | normalized current at maximum point |
| $v_{mp}$ | normalized voltage at maximum point |
| $\theta$ | calibration parameters |
| $K_{ph}$ | photocurrent ratio parameter |
| $K_0$ | saturation current ratio parameter |
| $K_{sh}$ | shunt resistance ratio parameter |
| $K_s$ | series resistance ratio parameter |
| $k_1$ | spectral ratio parameter |
| $Spl(\lambda)$ | splitting spectrum separation function |
| $Rs(\lambda)$ | spectrum response function |
| $Spe(\lambda)$ | solar irradiation spectrum function |
| $\alpha_{ph}$ | slope parameter of short-current and temperature |
| $\beta_{oc}$ | slope parameter of voltage and temperature |
| $E_g$ | band gap |
| $S$ | solar irradiation intensity |
| $S^{MRC}$ | solar irradiation intensity at MRC |

**Abbreviation**

| | |
|---|---|
| *MRC* | measurement reference conditions |
| *SRC* | standard reference conditions |
| *PV* | Photovoltaic |
| *TE* | Thermoelectric |

Reference


1. **M A. Green. 2004.** Recent developments in photovoltaics. *Solar Energy* . 76(1–3):3-8., 2004.
2. **Sah C T, Noyce R N, Shockley W. 1957.** Carrier Generation and Recombination in P-N Junctions and P-N Junction Characteristics. *Proceedings of the Ire.* 45(9):1228-1243, 1957.
3. **Moon R L, James L W, Vander Plas H A,. 1978.** Multigap solar cell requirements and the performance of AlGaAs and Si cells in concentrated sunlight. *13th Photovoltaic Specialists Conference.* 1978:859-867, 1978.
4. **Mojiri A, Taylor R, Thomsen E, et al. 2013.** Spectral beam splitting for efficient conversion of solar energy—A review. *Renewable & Sustainable Energy Reviews.* 28(28):654-663, 2013.
5. **Peters M, Goldschmidt J C, Löper P, et al.** Spectrally-selective photonic structures for PV applications[J]. *Energies*, 2010, 3(2): 171-193**.**
6. **Barnett A, Kirkpatrick D, Honsberg C, et al. 2009.** Very high efficiency solar cell modules. *Progress in Photovoltaics Research & Applications.* 17(1):75–83, 2009.
7. **Zhao Y, Sheng M Y. 2011.** Design of spectrum splitting solar cell assemblies. *Advances in Optoelectronics and Micro/nano-Optics. IEEE.* 1-3, 2011.
8. **Antonini A, Butturi M A, Zurru P, et al. 2015.** Development of a high/low concentration photovoltaic module with dichroic spectrum splitting. *Progress in Photovoltaics Research & Applications.* 2015, Vols. 23(9):1190-1201.
9. **Uzu H, Ichikawa M, Hino M, et al. 2015.** High efficiency solar cells combining a perovskite and a silicon heterojunction solar cells via an optical splitting system. *Applied Physics Letters.* 2015, Vols. 106(1):1433-1435.
10. **Li G, Shittu S, Diallo T M O, et al.** A review of solar photovoltaic-thermoelectric hybrid system for electricity generation[J]. *Energy*, 2018.
11. **Sonneveld P J, Glam S, Campen J, et al. 2010.** Performance results of a solar greenhouse combining electrical and thermal energy production. *Biosystems Engineering.* 2010, Vols. 106(1):48-57.
12. **Sonneveld P J, Swinkels G L A M, Tuijl B A J V, et al. 2011.** Performance of a concentrated photovoltaic energy system with static linear Fresnel lenses. *Solar Energy.* 2011, Vols. 85(3):432-442.
13. **Tian H, Mancilla-David F, Ellis K, et al. 2012.** A cell-to-module-to-array detailed model for photovoltaic panels. *Solar Energy.* 2012, Vols. 86(9):2695-2706.
14. **Chin V J, Salam Z, Ishaque K. 2015.** Cell modelling and model parameters estimation techniques for photovoltaic simulator application: A review. *Applied Energy* . 2015, Vols. 154:500-519.
15. **Cubas J, Pindado S, De Manuel C.** Explicit expressions for solar panel equivalent circuit parameters based on analytical formulation and the Lambert W-function[J]. *Energies*, 2014, 7(7): 4098-4115.
16. **A.Necaibia. 2012.** A Simple Theoretical Method for the Estimation of Dynamic Resistance in Photovoltaic Panels. *International Journal of Computer.* 45(14):21-25, 2012
17. **Chiacchio F, Famoso F, D'Urso D, et al.** Dynamic Performance Evaluation of Photovoltaic Power Plant by Stochastic Hybrid Fault Tree Automaton Model[J]. Energies, 2018, 11(2): 306.
18. **Karmalkar S, Haneefa S. 2008.** A Physically Based Explicit J-V Model of a Solar Cell for Simple

Design Calculations. *IEEE Electron Device Letters.* 2008, Vols. 29(5):449-451.

19. **Saleem H, Karmalkar S. 2009.** An Analytical Method to Extract the Physical Parameters of a Solar Cell From Four Points on the Illuminated J-V Curve. *IEEE Electron Device Letters.* 2009, Vols. 30(4):349-352
20. **Das, K.A. 2011.** An explicit J–V model of a solar cell for simple fill factor calculation. *Solar Energy.* 2011, Vols. 85(9): 1906-1909
21. **Das, K.A. 2014.** An explicit J–V model of a solar cell using equivalent rational function form for simple estimation of maximum power point voltage. *Solar Energy.* 2014, Vols. 98: 400-403.
22. **Lun S X, Du C J, Guo T T, et al. 2013.** A new explicit I – V, model of a solar cell based on Taylor's series expansion. *Solar Energy.* 2013, Vols. 94:221-232.
23. **Lun S X, Du C J, Sang J S, et al. 2014.** An improved explicit I – V, model of a solar cell based on symbolic function and manufacturer's datasheet. *Solar Energy.* 2014, Vols. 110:603-614.
24. **Laudani A, Fulginei F R, Salvini A. 2014a.** Identification of the one-diode model for photovoltaic modules from datasheet values. *Solar Energy.* 2014a, Vols. 108:432-446.
25. **Laudani A, Fulginei F R, Salvini A. 2014b.** High performing extraction procedure for the one-diode model of a photovoltaic panel from experimental I – V curves by using reduced forms. *Solar Energy.* 2014b, Vols. 103(103):316-326.
26. **Jain A, Kapoor A. 2004.** Exact analytical solutions of the parameters of real solar cells using Lambert W -function. *Solar Energy Materials & Solar Cells.* 2004, Vols. 81(2):269-277.
27. **Peters M, Goldschmidt J C**, Löper P, et al. Spectrally-selective photonic structures for PV applications[J]. Energies, 2010, 3(2): 171-193.
28. **Ju X, Xu C, Han X, et al.** A review of the concentrated photovoltaic/thermal (CPVT) hybrid solar systems based on the spectral beam splitting technology[J]. Applied Energy, 2017, 187: 534-563.
29. **Beeri O, Rotem O, Hazan E, et al.** Hybrid photovoltaic-thermoelectric system for concentrated solar energy conversion: Experimental realization and modeling[J]. Journal of Applied Physics, 2015, 118(11): 115104..
30. **Zhang Y, Gao S, Gu T. 2017.** Prediction of I-V characteristics for a PV panel by combining single diode model and explicit analytical model. *Solar Energy.* 2017, Vols. 144:349-355.
31. **Karmalkar S, Saleem H. 2009.** An Analytical Method to Extract the Physical Parameters of a Solar Cell From Four Points on the Illuminated J-V Curve. *IEEE Electron Device Letters.* 2009, Vols. 30(4):349-352.
32. **Karmalkar, S and Saleem, H. 2011.** The power law J–V, model of an illuminated solar cell. *Solar Energy Materials & Solar Cells.* 2011, Vols. 95(4):1076-1084.
33. **Pindado S, Cubas J, Roibás-Millán E, et al.** Assessment of Explicit Models for Different Photovoltaic Technologies[J]. Energies, 2018, 11(6): 1353.
34. **Soto W D, Klein S A, Beckman W A. 2006.** Improvement and validation of a model for photovoltaic array performance. *Solar Energy.* 2006, Vols. 80(1):78-88.
35. **Zeghbroeck, B. Van. 2011.** Principles of Semiconductor Devices. *Circuits & Devices Magazine IEEE.* 2011, Vols. 22(5):58-59.
36. **Radosavljevi, Radovan Lj, Vasi. 2012.** Effects of radiation on solar cells as photovoltaic generators. *Nuclear Technology & Radiation Protection.* 2012, Vols. 2012, 27(1):28-32.
37. **Breitenstein O, Rakotoniaina J P, Al R M H, et al. 2010.** Shunt types in crystalline silicon solar

 doi:10.20944/preprints201808.0248.v1

cells. *Progress in Photovoltaics Research & Applications.* 2010, Vols. 12(7):529-538.

38. **Ruschel C S, Gasparin F P, Costa E R, et al. 2016.** Assessment of PV modules shunt resistance dependence on solar irradiance. *Solar Energy.* 2016, Vols. 133:35-43.
39. **Reich N H, Sark, W.G.J.H.M. van, Alsema E A, et al. 2009.** Crystalline silicon cell performance at low light intensities. *Solar Energy Materials & Solar Cells.* 2009, Vols. 93(9):1471-1481.
40. **Khan F, Singh S N, Husain M. 2010.** Effect of illumination intensity on cell parameters of a silicon solar cell. *Solar Energy Materials & Solar Cells.* 2010, Vols. 94(9):1473-1476.